

Two Aerospace Corporation CubeSat Remote Sensing Imagers: CUMULOS and R3

Dee W. Pack
 The Aerospace Corporation
 2310 E. El Segundo Blvd., El Segundo, CA 90245; (310) 336-5645
 dee.w.pack@aero.org

David R. Ardila*
 Jet Propulsion Laboratory, California Institute of Technology
 4800 Oak Grove Dr., Pasadena, CA 91109; (818) 354-1855
 david.r.ardila@jpl.nasa.gov

Eric Herman, Darren W. Rowen, Richard P. Welle, Sloane J. Wiktorowicz, and Bonnie W. Hattersley
 The Aerospace Corporation
 2310 E. El Segundo Blvd., El Segundo, CA 90245

ABSTRACT

For remote sensing missions, the fractionated functionality of CubeSats provides a potential way to reduce cost and risks while maintaining comparable operational capabilities. This paper describes two CubeSat remote sensing missions developed by The Aerospace Corporation. The CubeSat Multispectral Observation System (CUMULOS) and R3 sensors will be hosted on 3U CubeSats developed by Aerospace. CUMULOS will research optimal methods for the operation of commercial off-the-shelf (COTS) camera sensors, and assess their ability to perform weather and environmental monitoring missions. The payload consists of three optics and sensor pairs: a panchromatic, visible CMOS camera, a short-wavelength infrared InGaAs camera, and a long-wavelength infrared microbolometer camera. These cameras are designed to operate in staring mode, and the payload will be able to capture images nearly simultaneously from the three cameras. CUMULOS is expected to launch no earlier than Fall 2017. R3 will demonstrate the ability of a 3U CubeSat to perform remote sensing activities analogous to Landsat 8's Operational Land Imager (OLI) instrument. The payload consists of a custom-designed refractive telescope combined with a filter block identical to those flown on Landsat 8, and a high-framerate commercial CMOS focal plane. Six of the nine Landsat 8 OLI bands will be read out. R3 will operate in a pushbroom mode, individual frames will be downlinked, and time-delay integration will be performed on the ground. This will be facilitated by an optical communications payload that will provide the necessary downlink. R3 is scheduled to launch no earlier than November 2017. Both payloads have been space-qualified on the ground by documenting their performance in a simulated space environment. The detectors' gain, point-response, non-uniformities, dark current, and non-linearity have been measured during pre-launch testing. Space-based vicarious calibration will be tied to Visible Infrared Imaging Radiometer Suite (VIIRS) and OLI.

INTRODUCTION

The Aerospace Corporation has built and flown more than 20 nanosats and picosats over the last 19 years with three completed systems waiting to be launched and several others in various stages of completion. These projects were each built upon lessons learned from its predecessors and incorporated improvements and risk reduction for the performance of the subsystems that all satellites share: power, communications, and attitude determination and control systems. Recent efforts have been aimed at launching more sophisticated payloads and sensors as technology demonstrators. Our experience with bus design allows for adaption and

compression of a great deal of mission capability into small CubeSat forms. This paper describes two sensors deployed in 3U CubeSats.

CUMULOS is a secondary, three-camera payload that was integrated onto the NASA/JPL Integrated Solar Array and Reflectarray Antenna (ISARA) mission. Bus sharing is a common practice on large spacecraft but less common on CubeSats. CUMULOS may be thought of as a miniature weather satellite with a special focus on low-light studies. A primary engineering research goal is to study the use and performance of commercially available uncooled infrared (IR) cameras in space.

*Work performed while employed by The Aerospace Corporation.

The second sensor, R3, is a multispectral pushbroom CubeSat. R3 may be thought of as a miniature Landsat 8 OLI, without the shortwave infrared (SWIR) bands.

Both 3U spacecraft buses rely on technology originally developed for prior AeroCube missions, in particular, the NASA Optical Communications and Sensor Demonstration (OCS-D, also termed AeroCube-7) spacecraft. The capability for precision pointing, necessary to demonstrate high-bandwidth laser communication on OCS-D, also finds application for these upcoming remote sensing missions: for precise point-and-stare imaging in one case (as well as the primary high-gain antennae test mission), and for precision control of yaw, pitch, and roll to enable time delay and integration (TDI) imaging in the other.

CUMULOS SENSOR AND MISSION

The CubeSat Multispectral Observation System (CUMULOS) is a secondary payload on the 3U CubeSat hosting the primary NASA/JPL ISARA mission. The CUMULOS payload was integrated on a non-interference basis and care was taken to ensure low risk to the primary payload mission. CUMULOS will research optimal methods for the operation of passively cooled COTS sensors and cameras and determine their suitability to perform weather and environmental

monitoring missions. The sections that follow briefly describe the primary ISARA mission, the spacecraft bus, the rideshare opportunity, and provide more detail on the CUMULOS payload, mission concept, and the expected performance.

Host Spacecraft and Payload

The primary payload of the host spacecraft is the Integrated Solar Array and ReflectArray antenna, which is a deployable Ka-band antenna designed to be compatible with a 3U CubeSat.¹⁻³ The ISARA antenna consists of three panels, each approximately 10 cm by 30 cm, that are hinged together and wrap around three faces of a 3U CubeSat during launch. After launch, the antenna is deployed as indicated in Figure 1 and provides a high-gain link with a ground station. The antenna is specifically designed to avoid the use of internal volume in the CubeSat. As such, once the satellite was fully designed to host the ISARA demonstration mission, there was over 1U of unused internal volume remaining. Figure 2 shows the internal structure of the ISARA satellite, with and without the CUMULOS payload, illustrating how the payload fits in space that was otherwise unused by the primary mission. The CUMULOS payload was designed to be hosted in this unused volume on a "do-no-harm" basis.

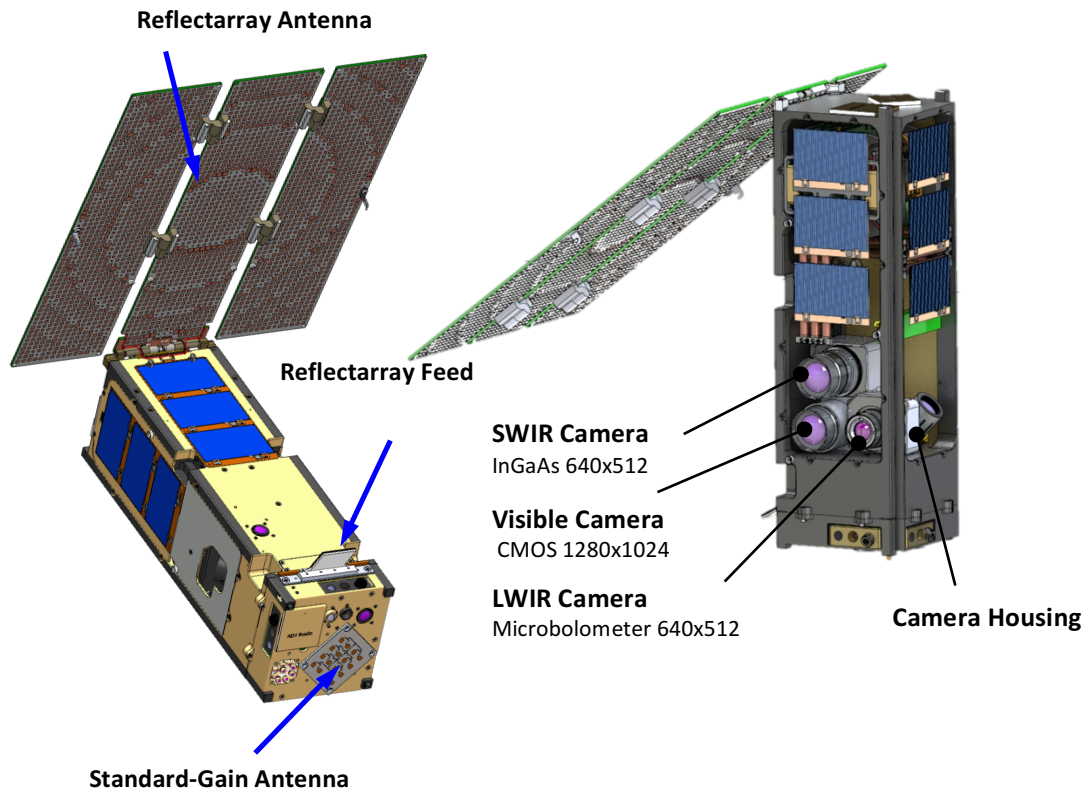


Figure 1: ISARA 3U spacecraft showing primary reflectarray and secondary remote sensing payloads

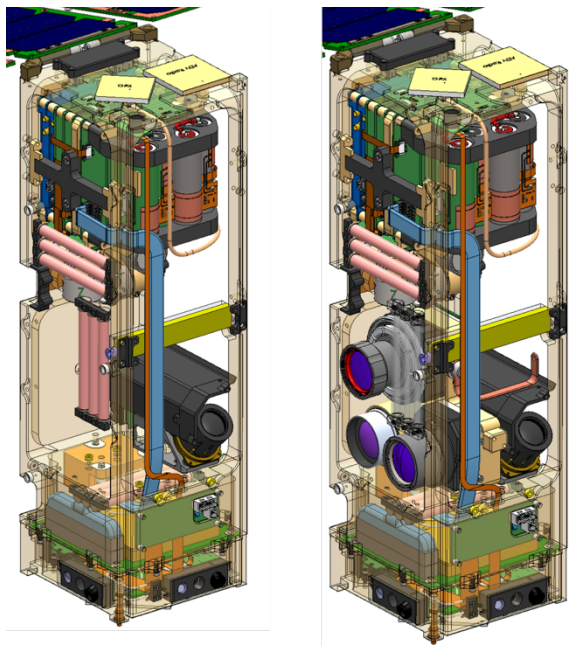


Figure 2: The ISARA spacecraft with and without the CUMULOS payload

In addition, the secondary payload will not be activated until the agreed-upon completion of the primary mission. The CUMULOS payload also will not impose any additional requirements on the bus beyond those necessary for the ISARA mission. As such, it will use the existing capabilities in power, attitude control, navigation, and communication that were developed for the ISARA mission.

Spacecraft Bus

Many of the systems of both the ISARA and R3 CubeSats are closely based on the AeroCube-7 OCSD 1.5U spacecraft, and use many of the same components. The ISARA bus is illustrated in Figure 3, which shows the location of the principal components. The standard bus avionics that are essentially identical to OCSD include a primary flight computer, two UHF radios, a GPS receiver for navigation, a dedicated attitude determination and control system (ADCS) processor, and a suite of ADCS sensors and actuators.

The primary flight computer is a PIC microcontroller that handles scheduling, state-of-health monitoring, and interfacing with the radios. The radios include a heritage 915-MHz ISM-band radio that Aerospace first flew on the PSSCT-2 mission in 2011. This radio (known as the ADV) has flown successfully on fourteen spacecraft, but is limited to a 500 kb/s

maximum downlink rate (200 kb/s is more typical). The second radio is a newly developed software-defined radio (SDR), also operating at 915 MHz, that first flew on the OCSD-A engineering model in 2015. This radio will allow up to 10x enhancement of the downlink rate. These two radios operate independently of one another, and each has its own antenna, providing a level of redundancy in the communication link. The navigation GPS receiver has a similar heritage to the ADV, having first flown on PSSCT-2.

The ADCS on ISARA is also very similar to that developed for OCSD. The OCSD ADCS was derived from the ADCS used in PSSCT-2, AC4, AC5, and AC8, but with significant upgrades. Most significant of the upgrades for OCSD was the addition of star cameras to provide precision pointing knowledge. This ADCS flew on the OCSD-A engineering model in 2015, but suffered a software error in the first week that disabled the ADCS processor. An extensive review of the software development process and software management processes led to changes that have been implemented in the OCSD flight units,^{4,5} as well as in ISARA. In addition to the star cameras, the ADCS upgrades for OCSD and ISARA included new

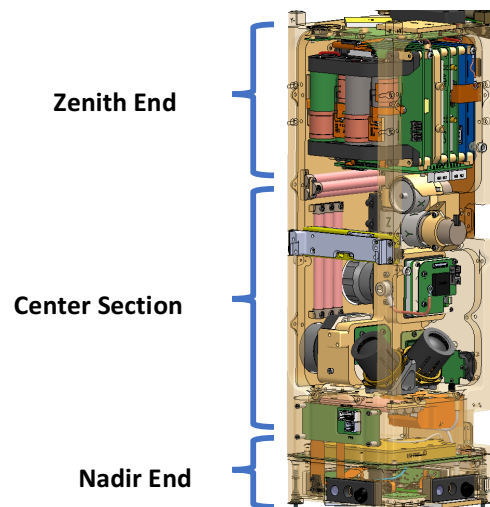


Figure 3: ISARA bus configuration. The Zenith end includes the avionics, the mounting of the reflectarray, and the batteries. The center section includes the ADCS sensors and actuators (star cameras, IMU, torque rods, and reaction wheels) as well as the wing release mechanism and the CUMULOS payload. The Nadir end includes the Ka-band feed and the standard-gain antenna, as well as the Ka-band tone generator.

Earth horizon sensors and additional sun sensors (one on each of the six spacecraft faces).

Because the ISARA spacecraft is three units in size and has a large deployable antenna, the reaction wheels used on OCSD (a 1.5U spacecraft) were determined to have insufficient control authority, so a new set of larger reaction wheels was developed. These wheels have 5.8 mN-m-s momentum storage capacity at a maximum rotation speed of 25,000 rpm. The development process included life testing and a detailed characterization of reaction wheel jitter.

The star cameras used for the ADCS are operated by a camera control board that was developed for OCSD and flew on the OCSD-A engineering model. Although the OCSD-A satellite is incapable of exercising any attitude control, much of the rest of the spacecraft, including the camera board, is fully functional. This board, as well as the two star cameras on the satellite, were tested in orbit and performed as expected⁵. The camera board is capable of operating up to five cameras. On ISARA, the primary mission requires the two star cameras, a nadir-facing camera for ADCS verification, and a camera to verify the deployment of the reflectarray. The bus camera board, in addition to managing camera operation, also does image processing on the star camera images to extract the star field data. These data are then sent to the ADCS board for star field matching and attitude determination. The CUMULOS payload includes three additional cameras, bringing the total on the spacecraft to seven, which could not be

accommodated with a single camera board. The camera board is self-compatible, however, making it possible to fly two camera boards on a single spacecraft. Thus, the CUMULOS payload has its own dedicated camera board.

The final heritage avionics board is the electric power system (EPS) that handles power conversion from the solar cells on the bus body, and provides power for all bus systems (and the CUMULOS payload). This EPS has flight heritage going back to AeroCube-4 in 2012, and has flown successfully on twelve spacecraft to date. However, this EPS is not capable of handling the high power level generated by the 24 solar cells arrayed on the back side of the reflectarray. A new high-power EPS was developed specifically for ISARA (called EPS-H) to handle this incoming power and provide power to the ISARA RF exciter.

Other than the EPS-H, the only new avionics board developed for ISARA was the payload interface board. This board routes power to the Ka-band exciter, controls the transmitter operation, and collects telemetry (power, thermal) from the payload. This payload interface board is dedicated to the primary payload, and is not involved in the operation of the CUMULOS payload. The avionics boards in ISARA are combined into a single stack, as illustrated in Figure 4. This configuration facilitates integration and testing of the avionics as a complete package prior to integration of the satellite as a whole.

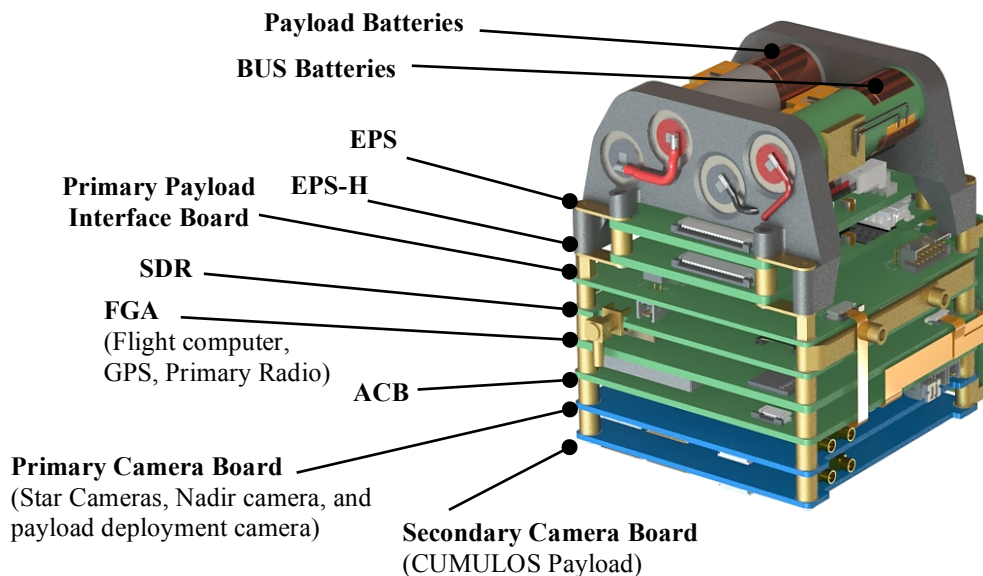


Figure 4: ISARA avionics stack

The CUMULOS payload, as noted, is controlled through a second camera board located at the bottom of the stack. In the interest of mission assurance for the primary payload, the CUMULOS payload will not be activated until completion of the primary mission. To ensure that the CUMULOS cameras do not interfere with the primary mission, the CUMULOS camera board, which is not required for the primary mission, is powered through a separate, switched, power circuit from the EPS. The cameras, in turn, can be turned on by the CUMULOS camera board, on command from the flight computer. Any unintended operation of the CUMULOS cameras would require two separate commands: one to power the CUMULOS camera board, and one to switch on the cameras after power is applied to the camera board.

ISARA Rideshare Opportunity

In 2014, The Aerospace Corporation proposed an idea for a secondary payload to fill approximately 1U of unused volume on the ISARA spacecraft. The primary ISARA mission required a 3U bus to accommodate the reflectarray antennae/solar panel structure, but used less than 2U of spacecraft volume. To fill the remaining volume, we chose the combination of two readily available compact uncooled IR cameras, and a visible camera similar to those flown on prior AeroCube missions, but with greater low-light sensitivity. The Space and Missile System Center's Advanced Development program office (SMC/AD) was interested in gaining experience with flying COTS camera hardware and funded the secondary payload effort. The sensor capabilities matched specific nighttime remote sensing science goals of The Aerospace Corporation's Space Science Applications Laboratory, including exploring the utility of the near infrared for nighttime cloud detection and combining cloud and nightlight sensors on a single payload.⁶ Payload development was greatly speeded by use of the 5-camera controller card technology for the OCS/D/AC-7 satellite. Some added software was necessary for this card to control the new cameras. Power conditioning boards were also necessary for the IR cameras. As mentioned above, two camera cards were necessary, as the main payload had two star sensors, a nadir-pointed fisheye camera, and a reflectarray deployment fisheye camera. Redundant boards also ensured there was less risk to the main reflectarray experiment. The new imaging instruments were as isolated as possible from the primary experiment.

CUMULOS Payload

Three separate cameras comprise the CUMULOS payload: 1) a visible (VIS) CMOS camera, 2) a SWIR,

InGaAs camera, and 3) a longwave infrared (LWIR), vanadium oxide microbolometer. The VIS camera uses an Aptina MT9M001C12STM CMOS chip mated to a ruggedized Schneider Xenoplan lens. The SWIR camera is a FLIR Tau SWIR 25 equipped with a vented lens from Stingray Optics. The LWIR camera is a FLIR Tau 640 using the vendor's lens choice. The visible and LWIR cameras are passively cooled. The SWIR focal plane is temperature stabilized using an internal thermo-electric cooler (TEC). The cameras underwent TVAC and vibration testing independently, and with the integrated ISARA payload. Basic calibration tests such as darks, flat fields, linearity and modulation transfer function (MTF) measurements were performed.⁷ Together, the sensors will be used as a small-aperture, staring payload suitable for testing the performance of passively cooled sensors to perform space-based weather and environmental monitoring missions. The sensor specifications are shown in Table 1. The host spacecraft was originally scheduled to be placed in 575 km circular, 97.7° inclination, sun-synchronous orbit with a 10:30 am equatorial crossing time by a Falcon 9 launch vehicle. Late breaking decisions may enable an earlier launch on the OA-8 ISS resupply flight during Fall, 2017. In this option, after a 6-week dock, the upper stage would then place the host spacecraft into a 500-km circular orbit with 52° inclination. The orbit-dependent terms in Table 1 and Figure 5 will change a bit as a result.

Table 1: CUMULOS Sensor Specifications

Sensor Specifications	CUMULOS VIS	CUMULOS SWIR	CUMULOS LWIR
Lens f-number	1.4	1.4	1.1
Lens focal length (mm)	17.6	25	25
Pixel Pitch (µm)	5.2	25	17
Spectral Band (µm)	0.4 - 0.8	0.9 - 1.7	7.5 - 13.5
Quantization (bits)	10	14	14
Integration time (ms)	0.11 - 900	0.18 - 32	not appl. 10-ms time constant, 30 Hz max
Sensor Vendor Type	Aptina Si CMOS	FLIR InGaAs	FLIR VOx microbolometer
Array Size	1280x1024	640x512	640x512
Nominal Alt. (km)	575	575	575
GSD (m)	170	575	391
Approx. Image Footprint (km)	218 x 174	368 x 294	250 x 200
Repeat Cycle (days)	14	8	11

Mission Concept

CUMULOS is designed to be used as a staring sensor. The basic collection sequence involves taking an image triplet, one frame per camera, as fast as possible to cover a region of interest. Figure 5 shows the pixel

and swath of each camera projected onto the Los Angeles region. CUMULOS will obtain near-simultaneous frames with the three cameras. The individual cameras can frame rapidly, but downlink constraints will direct our focus towards taking small numbers of frames from each camera on selected targets of interest. With our current groundstation capabilities we can downlink one to two raw-file image triplets per ground-station contact. During operations, we will downlink thumbnail images and then select which full-frame JPEGs or raw files to retrieve from the 8-GB on-board storage. More full frames may be downlinked if JPEG compression and/or pixel aggregation are used. Use of the SDR radio, currently being tested on AC-7A, increases data downlink rates by a factor of 4. Note that the ISARA antenna is not connected to a radio, so we can't take advantage of its high gain capabilities with CUMULOS.

CUMULOS will leverage the improved pointing capabilities of the current generation Aerospace Corporation CubeSat bus, and add multispectral capabilities, to advance the point-and-stare nighttime imaging experiments we previously initiated with the visible cameras on AeroCube-4, 5, and 8.^{6,8} The three cameras were chosen for nighttime sensitivity and, in the case of the microbolometer, to test an uncooled microbolometer as a cloud and land surface temperature sensor. Remote sensing applications to be investigated include: cloud detection and characterization, land and water surface temperature measurement, urban heat island measurement, hotspot detection (fires, gas flares, and volcanic activity), and nightlight detection with both the VIS and SWIR sensors. Attempts will be made to image dynamic

weather events. While the nominal repeat cycles for all cameras are listed in Table 1, pointing off-nadir will allow more frequent revisit times. Particular attention will be paid to imaging weather at night to research capabilities similar to the VIIRS day/night band (DNB). The visible and SWIR cameras will be capable of imaging the Earth's surface and clouds when illuminated by moonlight and the airglow. The SWIR 0.9 to 1.7 μm band spans many excited OH emission lines in the atmospheric airglow (the Meinel bands). Much more illumination falls in the SWIR band than in the weak visible emissions detected by the VIIRS DNB under zero moonlight conditions in prior work.⁹ We want to study the utility of the wide-open SWIR band for weather missions and gain experience that can be applied to future weather sensors. The thermal waveband will be used to track cold clouds in the upper atmosphere as well as forest fires on the Earth's surface. Comparisons between bands will aid in performance assessment. Comparisons of CUMULOS data to VIIRS, Moderate-resolution imaging spectroradiometer (MODIS), and Defense Meteorological Satellite Program (DMSP) data, as well as data from the Japanese Space Agency Compact Infrared Camera (CIRC)¹⁰ and related on-orbit microbolometers, will be conducted to validate performance.

Calibration verification and on-orbit performance analysis are key parts of the mission goal of testing performance of commercial sensors. Radiometric calibration will be obtained from observations of stars, the Moon, and the Earth, and will be tied to that of other space sensors. Stellar observations with the VIS and SWIR sensors will be used to measure the operational point spread function.



Figure 5: Pixel footprints and fields of view for the three CUMULOS cameras projected onto The Aerospace Corporation and the Los Angeles region. The cameras are co-boresighted.

Expected Performance

The calibration and performance of the CUMULOS sensor was summarized by Ardila in 2016.⁷ Figure 6 shows some performance metrics with an emphasis on what the system will see. The VIS and SWIR cameras will both have good nighttime sensitivity with the ability to see the moonlit Earth and clouds. Some capability is expected by the SWIR to detect OH airglow emission in the Mienel bands and, possibly, airglow illuminated clouds. Both the VIS and SWIR cameras will have excellent capabilities to detect nightlights and hotspots during nighttime observations. Based on our TVAC observations of cold blackbodies, the LWIR microbolometer camera will detect sources with temperatures close to -60°C. This will allow for detection of cloud structure for warm clouds. Higher-altitude, colder clouds will appear as "holes" in contrast against the warmer Earth and ocean surface.

R3 SENSOR AND MISSION

Spacecraft Bus

The R3 spacecraft bus is very similar to the ISARA bus, with some changes to accommodate the different payload. It does not have the deployable reflectarray used on ISARA, but has instead two deployable solar panels for power generation, as illustrated in Figure 7. All of the non-payload avionics boards are nominally identical to those used for ISARA. R3 has a total of four cameras; the two star cameras, the primary payload camera, and a small nadir-facing camera used for ADCS verification and to provide context images for the primary payload. As such, the R3 avionics stack includes only one camera board. The payload interface board developed for R3 does not reside in the avionics stack, but is located near the optical telescope.

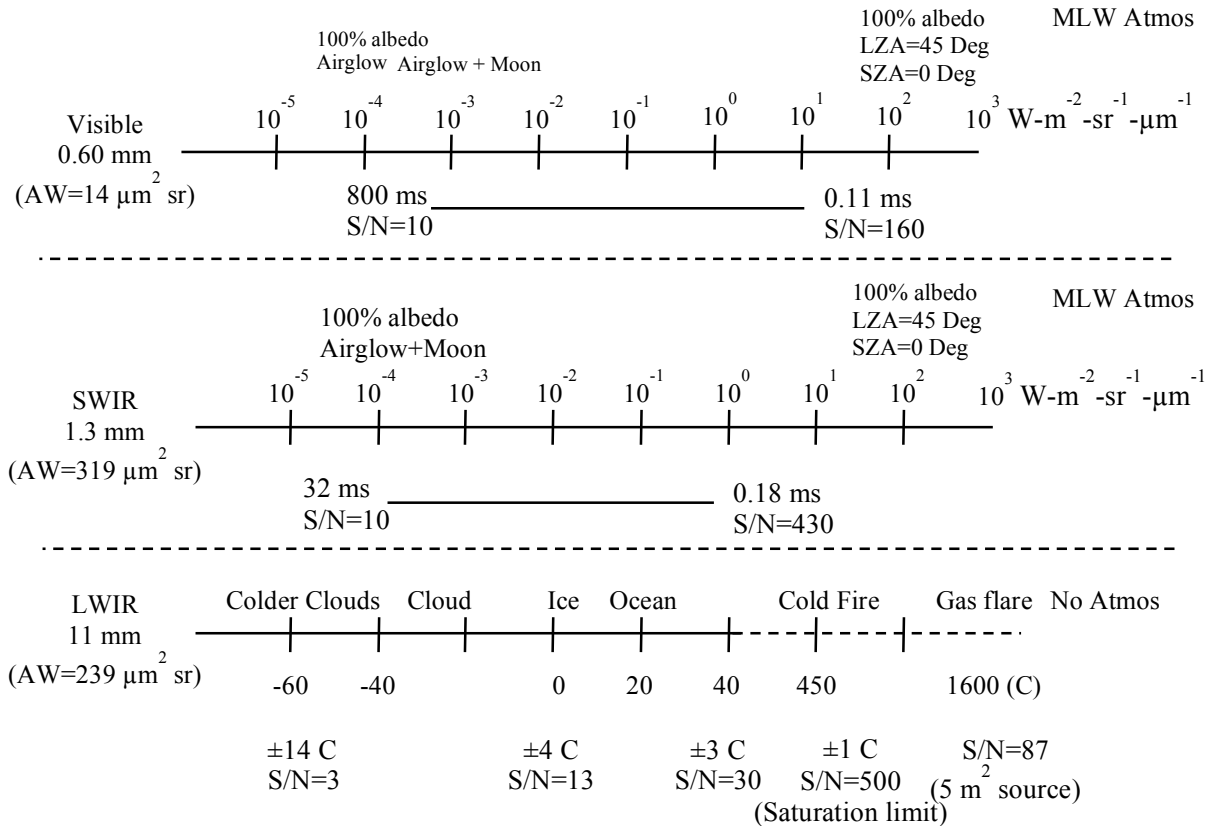


Figure 6: Expected performance for the three CUMULOS cameras

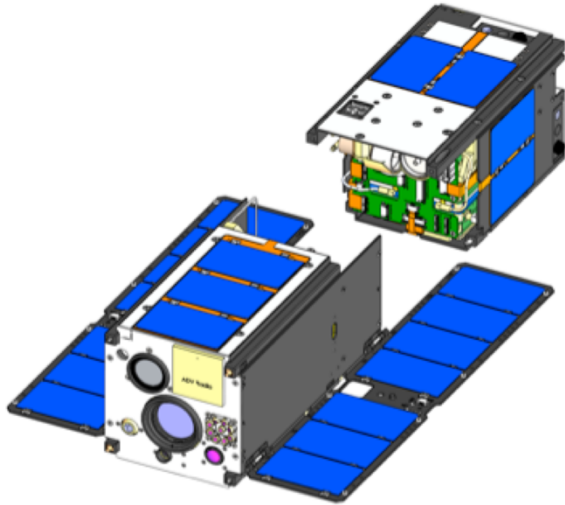


Figure 7: R3 satellite showing the line of assembly between the payload and avionics sections

In addition to the standard suite of avionics, the R3 spacecraft bus includes a communication laser very similar to the OCS design, but incorporating some design changes based on experience gained in building the OCS flight lasers. Specifications are unchanged from OCS, with an operating wavelength of 1064 nm, 3 W output power, and a beam divergence of 0.05°. It is expected that this laser will be able to provide up to a 200 Mb/s downlink capacity. The design developed for OCS used the camera board to interface with the laser, and this is continued in R3.

Two other design changes relative to ISARA are noteworthy. First, while the ISARA spacecraft used star cameras identical to those developed for OCS, including deployable sun shields, the star cameras in R3 use an updated design with fixed sun shields. The focal plane array (FPA) and all associated electronics remain unchanged, however.

The second design change is in the method of manufacture. All satellites in the AeroCube series, as well as ISARA, use a single-piece outer shell for the spacecraft body. This shell incorporates the launch rails and side walls (but not the end faces), and is fabricated from a single piece of aluminum using wire electrical discharge machining (EDM) to cut out the internal volume. All internal components of the spacecraft are assembled through the two ends. This process was used both to provide structural rigidity, and to ensure good electrical conductivity around the shell to promote eddy-current dissipation for passive detumbling. In ISARA, all of the outer shell, except for the wall around the Ka-band exciter electronics near the nadir face, was made from a single piece of aluminum in this manner. Experience with ISARA

taught us that assembling an entire 3U satellite through the endcaps presented a serious integration challenge, so the design was modified in R3 to break the shell into two halves, as illustrated in Figure 7, where the two halves of the satellite are shown separately. In this configuration, both halves of the satellite are still encased in solid shells fabricated using wire EDM, ensuring there is excellent structural rigidity and good eddy-current dissipation. Both halves of the satellite are fabricated primarily by insertion of components along the z axis, and the final assembly involves mating the two halves together with appropriate electrical interconnects.

R3 Payload

The R3 payload was designed to collect multispectral imagery similar to that of Landsat-8 OLI from a 3U satellite. The payload consists of a refractive optical telescope paired with a COTS FPA. Multispectral data are collected with a bandpass filter overlaid onto the FPA operating as a push-broom imager. The filter was provided by Materion Precision Optics and is identical to those used on Landsat-8. Only the visible bands and one NIR band are used (Table 2). Within each spectral band, 17 pixel rows are read out. In the panchromatic band, 8 pixel rows are read out. Data for each band are co-added on the ground to provide TDI. Due to the constraints of fitting a payload and bus into a 3U satellite, SWIR bands were excluded from the design, leaving the VIS and near-infrared (NIR) bands, which are imaged using a single silicon focal plane array. The focal plane is an ON Semiconductor LUPA 1300-2 CMOS chip which was chosen for its high framerate capabilities, low noise characteristics, and our previous experience with related chips.

Table 2: R3 Filter Wavebands

Landsat Band	Band Name	Wavelength
1	Coastal / Aerosol	0.43 – 0.45 μ m
2	Blue	0.45 – 0.51 μ m
3	Green	0.53 – 0.59 μ m
4	Red	0.64 – 0.67 μ m
5	Near Infrared	0.85 – 0.88 μ m
8	Panchromatic	0.50 – 0.68 μ m

The configuration of the spectral filters and the constraints of the satellite size led to the optical requirements in Table 3. The waveband, f-number, and telecentricity were predetermined by the spectral filter. The entrance pupil diameter and track length requirements were driven by packaging constraints within the entire satellite. The final payload optical performance requirement is based upon both rule-of-thumb for minimum resolvable contrast levels and the Nyquist frequency of the pixels.¹¹

Table 3: R3 Payload Optical Requirements

Requirement	Value
Waveband	0.43 – 0.89 μ m
Entrance Pupil Diameter	25mm
f-number	6.4
Image Height	11.5mm
Pixel Pitch	14 μ m
Track Length	< 200mm
Telecentricity	< 1°
MTF Performance	>20% contrast at Nyquist frequency

A trade study was performed to determine whether a COTS lens would be acceptable for this program. Despite the cost benefit, we determined the requirement non-conformances in the identified COTS lens were too great to be accepted. COTS optical lenses typically operate within the VIS waveband only. Excluding the NIR band would have decreased the utility of the sensor and was unacceptable. In addition, the prevalence of bonded optical elements within the COTS lens added risk. The space environment can cause debonding within optical elements over time due to stresses in the different coefficients of thermal expansion (CTE).¹² X-ray imaging confirmed the presence of three bonded doublet elements in the candidate COTS lens. Due to the presence of bonded optical elements, spectral performance range, and non-space-qualified focus mechanism lubrication, the candidate COTS lens was rejected.

The path forward from the trade study was to design an optical telescope that would meet the requirements in Table 3, while still being cost effective and reducing risk. Ideally, a reflective design would have been chosen based on the waveband requirements. A deterrent from reflective designs in this case was the wide field-of-view in a tight packaging constraint. A three mirror anastigmat (TMA), for example, could meet the requirements of this system, but would have required a much larger packaging volume. For refractive designs, the literature suggested a Petzval configuration.^{13,14} This design proved optimal in correcting for chromatic aberration and meeting the packaging constraints while maintaining telecentricity.

The optical design that was used for R3 is shown in Figure 8. In this optical design, the first two lens elements need to be bonded or very close together. Our design execution made sure that a reasonable spacing could keep these two elements close enough for chromatic correction without needing to be bonded.

The opto-mechanical design for the telescope aimed to ease assembly in addition to satisfying the primary imaging requirements. The opto-mechanical layout is shown in Figure 9. We chose a single-bore drop-in configuration.¹⁵ This configuration minimized the ground support equipment (GSE) needed to install each optical element, met the requirements of the optical system, and reduced the potential cost of additional opto-mechanical components.^{16,17}

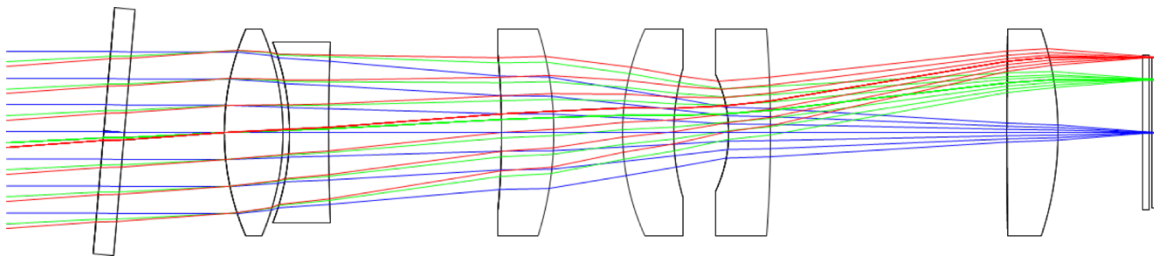


Figure 8: Optical layout of the R3 telescope

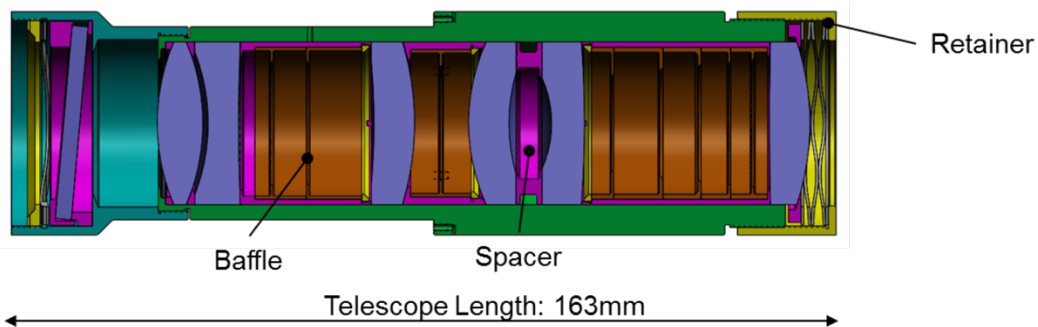


Figure 9: Opto-mechanical layout of the R3 telescope

Figure 10 shows the method of integration used with the GSE to support the assembly process. A subcell assembly spacer was designed to ensure that tolerance stack-ups were not a concern, while reducing stray light. The subcell assemblies were also designed to reduce stray light paths by including vanes.



Figure 10: Assembly of optical telescope utilizing ground support equipment to ease installation

The payload was required to operate from -30°C to $+70^{\circ}\text{C}$. This temperature range was too large to perform the athermalization correction optically. A focus mechanism was implemented for thermal correction over this entire temperature range. The focus mechanism uses a motor and gear system to move the telescope axially relative to the focal plane. The mechanism implements a cam scheme to control the movement amount relative to the rotation of the telescope. The encoder counts of the motor were matched to the axial movement the telescope required for thermal correction. A sketch of the telescope and focus mechanism can be seen in Figure 11.

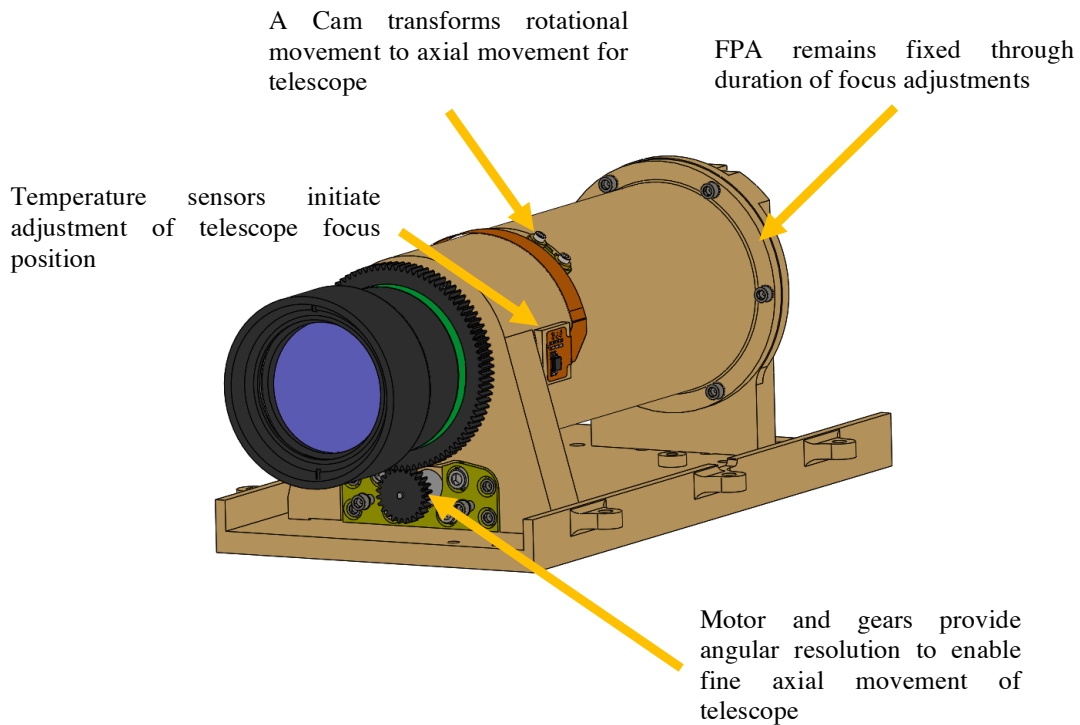


Figure 11: Payload focus mechanism to adjust optical focus position relative to temperature

The complexity of each subassembly within the payload made it necessary to perform extensive testing prior to payload integration. Given the design, it was possible to easily install each subassembly within the payload following individual tests. These procedures were similar to the way COTS components are treated in a plug-and-play system. This process followed the example of many CubeSat programs in their methods of implementing components.

Following the integration, payload level testing incorporated environmental conditions and functional testing. The payload was put through thermal vacuum (TVAC) testing while optically imaging a test pattern. The test pattern was a slanted knife edge to acquire the MTF through post-processing. Images that were taken throughout the TVAC test validated the focus mechanism performance. MTF measurements were taken at different temperatures, which allowed for correlation between the telescope position (relative to the focal plane) and the surrounding temperature. A model of this correlation was converted into a look-up table to command the focus mechanism on-orbit. More details on the optical and radiometric testing will be presented at the AIAA/USU Conference on Characterization and Radiometric Calibration for Remote Sensing in August 2017.¹⁸

Table 4 summarizes the sensor specifications including important focal plane parameters. The sensor frame rate, GSD, swath width, and revisit are determined by the 500 km orbit. The sensor and

spacecraft could perform in higher or lower orbits with no mechanical or software modifications other than changing the frame rate to match the orbital velocity.

Mission and Operations

R3 is an engineering demonstration with the mission of performing remote sensing activities analogous to the Landsat 8 OLI instrument. These activities include vegetation health, water quality and land use monitoring, and aerosol characterization. We will assess R3 data quality and our ability to perform on-orbit calibration and vicarious calibration against the OLI and related sensors.

We will perform stellar observations as well as measurements of dark regions of space and uniform flat terrestrial playas. We will use these for on-orbit calibration and will assess the results when compared to ground calibration. We will pursue collaboration and data comparisons with other satellite researchers who are interested in cross-calibration and joint studies.

Initial operations will consist of collecting multi-frame image strips to assess our ability to fly the sensor properly oriented along the focal plane to co-add frames for TDI imagery. Automated collection of 1 image strip per day or more will follow as automated laser downlink operations are developed. The current laser groundstation will allow for approximately 23 spectral images per pass to be downlinked (where a spectral image has a dimension of 1280 pixels cross track, 1000 along track, 6 spectral channels). The SDR allows for up to 0.3 spectral images per pass to be downlinked, and we model an average of 11 contacts with our current RF groundstations, so some data may be brought down via this radio. The ADV radio is not suited for downlinking 1000s of frames of multispectral data. On-board TDI would reduce the data rate by a factor of 15, but this is not implemented in our current design.

Expected Performance

Models of the payload performance predict that the signal-to-noise ratio (SNR) for each of the 6 Landsat bands will be within 10% of OLI performance. We recently concluded detailed calibration testing. Some issues not included in the model, such as focal plane electrical offsets, are now being accounted for, which may impact the SNR. Results will be presented at the AIAA/USU Conference on Characterization and Radiometric Calibration for Remote Sensing in August 2017.¹⁸

Table 4: R3 Sensor Specifications

Sensor Specifications	R3
Lens f-number	6.4
Lens Focal Length (mm)	160
Pixel Pitch (μm)	14
Spectral Bands # (μm)	6 (0.43-0.89)
Quantization (bits)	10
Integration Time (ms)	1.0 nominal, 0.1-1.8 for daytime albedos (up to 125 possible)
Frame Rate (hz)	181.2 nominal
Array Size	1280x1024 (1280x91 read out)
Nominal Alt. (km)	500
GSD (m)	44
Swath Width (km)	56
Repeat Cycle (days)	47

OPPORTUNITIES FOR RESEARCH AND COLLABORATION

A number of commercial and government efforts are underway to study weather, disaster mitigation, fire detection and land surface characterization with CubeSats and SmallSats. We welcome opportunities for joint experiments and collaborations as we demonstrate the new CUMULOS and R3 sensor capabilities in orbit. Some experiments that are hard to perform on large operational spacecraft, such as using sensors in non-standard modes, varying integration times, interrupting standard collection modes to point off-nadir, exploring new bands and uses of existing bands, and exploring non-standard calibration techniques, are facilitated with CubeSats. We are interested in collaborating with VIIRS and Landsat researchers to perform observations that are not currently possible with those systems using our CubeSat sensors as testbeds.

CONCLUSION

CUMULOS and R3 mark our initial efforts towards integrating more complex remote sensing payloads on CubeSats for remote sensing research and to investigate optimal methods of calibrating small sensors on orbit. Two missions were chosen for development: a weather and nighttime environmental monitoring experiment using COTS cameras, and a custom-built multi-spectral VIS and NIR landcover sensor. Future progress in remote sensing with CubeSats will depend upon the further development of compact payloads and more capable, possibly larger buses (6U) equipped with high-speed data downlinks. Both the ISARA/CUMULOS efforts and the R3 effort will contribute towards advancing the state-of-the-art when they achieve orbit, and to demonstrating the impressive capabilities of modern small spacecraft.

Acknowledgements

This research was funded by The Aerospace Corporation's Independent Research and Development program. The authors wish to acknowledge the U.S. Air Force Space and Missile Systems Center Advanced Development Directorate (SMC/AD) for their support of the CUMULOS payload.

Special thanks to Kevin Downing at Materion Precision Optics for providing the filter array used in the R3 payload. The filters provided are identical to those used on the OLI instrument on Landsat 8. Their assistance with this project was critical.

The authors would like to thank the NASA Small Spacecraft Technology Program and the Jet

Propulsion Laboratory ISARA team for the inclusion of the CUMULOS secondary payload on the ISARA spacecraft.

David Ardila performed his work on both the CUMULOS and R3 projects, while employed at The Aerospace Corporation, prior to joining the Jet Propulsion Laboratory.

References

- [1] Hodges, R. E., Shah, B., Muthulingham, D., Freeman, A., "ISARA Mission Overview," Proc. 27th Annu. AIAA/USU Conf. Small Satell. SSC13, SSC13-WK-19 (2013).
- [2] NASA Jet Propulsion Laboratory., "Integrated Solar Array & Reflectarray Antenna (ISARA)," 2015, <https://www.jpl.nasa.gov/cubesat/missions/isara.php> (15 May 2017).
- [3] Hodges, R. E., Hoppe, D. J., Radway, M. J., Chahat, N. E., "Novel Deployable Reflectarray Antennas for CubeSat Communications," 2015 IEEE MTT-S Int. Microw. Symp., 1-4, Phoenix, AZ (2015).
- [4] Janson, S. W., Welle, R. P., "The NASA Optical Communication and Sensor Demonstration Program," Proc. 27th Annu. AIAA/USU Conf. Small Satell. SSC13, SSC13-II-1 (2013).
- [5] Janson, S. W., Welle, R. P., Rose, T. S., Rowen, D. W., Hardy, B. S., Dolphus, R., Doyle, P., Faler, A., Chien, D. H., et al., "The NASA Optical Communications and Sensor Demonstration Program: Initial Flight Results," Proc. 30th Annu. AIAA/USU Conf. Small Satell. SSC16, SSC16-III-03 (2016).
- [6] Pack, D. W., Hardy, B. S., "CubeSat Nighttime Lights," Proc. 30th Annu. AIAA/USU Conf. Small Satell. SSC16, SSC16-WK-44 (2016).
- [7] Ardila, D. R., Pack, D. W., "The CubeSat Multispectral Observation System (CUMULOS)," Proc. Conf. Charact. Radiom. Calibration Remote Sens. (2016).
- [8] Pack, D. W., Hardy, B. S., "Studying the Earth at Night from CubeSats", Proc. 31st Annu. AIAA/USU Conf. Small Satell. SSC17, SSC17-WK-35 (2017).
- [9] Miller, S. D., Mills, S. P., Elvidge, C. D., Lindsey, D. T., Lee, T. F., Hawkins, J. D., "Suomi satellite brings to light a unique frontier of nighttime environmental sensing capabilities," Proc. Natl. Acad. Sci. United States Am. **109**(39), 15706-15711 (2012).

- [10] Kato, E., Katayama, H., Sakai, M., Nakajima, Y., Kimura, T., Nakau, K., Tonooka, H., "Initial Checkout Results of the Compact Infrared Camera (CIRC) for Earth Observation," Proc. 36th Int. Symp. Remote Sens. Environ. XL-7/W3, 1215–1220 (2015).
- [11] Friedman, E., Miller, J. L., [Photonics Rules of Thumb: Optics, Electro-Optics, Fiber Optics, and Lasers], 2nd ed., SPIE Press, Bellingham (2004).
- [12] Sinclair, D., Enright, J., Dzamba, T., Sears, T. M. C., "Custom Optics vs Modified COTS for Small Spacecraft: The Build vs. Rebuild Decision," Proc. AIAA/USU Conf. Small Satell., SSC15-VII-2 (2015).
- [13] Smith, W. J., [Modern Lens Design], 2nd ed., McGraw-Hill, New York (2005).
- [14] Bentley, J. L., Olson, C., [Field Guide to Lens Design], 1st ed., SPIE Press, Bellingham (2012).
- [15] Yoder, P. R., [Mounting Optics in Optical Instruments], 2nd ed., SPIE Press, Bellingham (2008).
- [16] Herman, E., "Optical Design in the Age of CubeSats," Proc. SPIE, in prep. (2017).
- [16] Herman, E., "Optical Design in the Age of CubeSats," Proc. SPIE, in prep. (2017).
- [17] Herman, E., Vore, A. G., Tardif, J., Fuller, J., "Commercial tolerancing and assembly for space-based optical missions," Proc. SPIE 10377, in prep. (2017).
- [18] Wiktorowicz, S. J., Russell, R. W., Pack, D. W., Herman, E., Rossano, G. S., Ardila, D. R., Coffman, C. M., Hardy, B. S., Hattersley, B. W., "Calibration of the AeroCube-11 Focal Plane Array", Conf. Charact. Radiom. Calibration Remote Sens. in prep. (2017).